International Journal of Future Generation Communication and Networking
Vol. 8, No. 1 (2015), pp. 215-226
http://dx.doi.org/10.14257/ijfgcn.2015.8.1.22

An Application of Fiber-Connected Distributed Antennas to Heterogeneous Networks: Energy Efficiency Perspective

Ying Sun[1], Yuxian Huang[1] and Liming Chen[2]*

[1]*Guangzhou Power Supply Company, China Southern Power Grid, Guangzhou, China 510080*
[2]*Electric Power Research Institute, China Southern Power Grid, Guangzhou, China 510080*
*sunying@csg.cn, huangyx@csg.cn, *chenlm2@csg.cn*

Abstract

Fiber-connected distributed antenna systems (DAS) have been recognized as an effective means to accommodate the coverage and capacity demands of future heterogeneous networks (HetNet). Among various opportunities realized by the architecture, our focus in this paper is on the spectral efficiency (SE) advantages achieved by cooperative transmission and the associated power consumption that may affect the energy efficiency (EE) of the system. A detailed power model is developed to benchmark the various sources of energy consumption in fiber-connected DAS. Then a simple but efficient pre-coding scheme is proposed to reduce the computation complexity associated with cooperative transmission, thus lowering the power consumed by baseband processing while at the same time maintaining a high throughput performance. Through detailed and extensive simulations, this paper demonstrates the SE and EE advantages of the application of fiber-connected DAS in HetNet.

Keywords: *heterogeneous networks; fiber-connected distributed antenna system; cooperative transmission; power consumption; energy efficiency;*

1. Introduction

The explosive growth of mobile wireless traffic, fuelled by the proliferation of internet-connected devices and the variety of bandwidth consuming services demanded by end users, inspires and challenges the design of future heterogeneous networks (HetNets), which consists of overlapped macro- and femtocells in the same area. Fiber-connected distributed antenna systems, which integrates the advantages of a distributed antenna system (DAS) with centralized processing capability connected through an optical fiber medium, emerges as a promising solution to address the increased network capacity demand [1, 2]. This network architecture leverages conventional inter-cell interference to improve the signal quality on the downlink at cell boundaries and enhance signal reception at base stations (BSs) for the uplink by allowing several BSs to cooperate in transmitting/beam-forming a signal to (or receiving and jointly processing a signal from) mobile users, which leads to significant improvements in the capacity and spectral efficiency (SE) of cellular systems [3, 4].

With the growing "green" concern over energy consumption and environmental effects, energy efficiency (EE) of fiber-connected DAS was recently paid much attention [5-7]. In [6], the tradeoff between EE and SE in downlink DAS was investigated and a constrained optimization problem was solved to maximize EE through proposed power allocation scheme under the SE requirement and maximum power limit. In [7], an energy efficient power allocation scheme was proposed to minimize the Joule consumed per bit for frequency selective fading environment in downlink DAS. However, the cooperative

ISSN: 2233-7857 IJFGCN

techniques considered by these studies mitigate co-channel interference through beam-forming utilizing whole channel state information (CSI) among users and BSs, which generates explosive computation complexity at the central processing unit. This complexity directly translates into prohibitive power consumption, and, if not carefully addressed, would lead to decreased EE. Therefore, a comprehensive solution that covers the challenging tasks of investigating the power consumption of fiber-connected DAS and reducing the computation complexity while maintaining a high SE performance is yet to be proposed. Furthermore, the solution would also be desirable to other emerging HetNet architectures, such as Cloud based Radio Access Network (C-RAN) [8-9], whose general purpose processor based central signal processing currently faces the challenges of much slower signal processing and lower power efficiency in comparison with dedicated processors.

In this paper, we address the above mentioned EE problem in downlink HetNets which adopt fiber-connected distributed antennas to replace the macro- and femtoBSs, focusing on reducing the power consumption incurred by cooperation associated computation complexity, *i.e.*, full channel matrix inversion required by beam-forming (*e.g.* zero-forcing) and power allocation under the per-antenna power constraint, while maintaining a satisfactory SE. To get detailed analysis of the power consumed by each element of the network, we first introduce a comprehensive power model by deconstructing the total consumed power into separate parts. A simplified pre-coding scheme is then proposed to reduce the computation complexity of channel matrix inversion and power allocation, which consequently drops the energy consumption of the baseband processing. Numerical results under different coverage scenarios are given to demonstrate the satisfactory SE and EE performance of the fiber-connected DAS with proposed scheme in HetNet.

The rest of this paper is organized as follows: In Section 2 we describe the EE of fiber-connected DAS and the power consumption of each system component. In Section 3 we spell out the details of our proposed pre-coding scheme for downlink cooperative transmission. Numerical results are presented in Section 4 and concluding remarks are given in Section 5.

2. EE of Fiber-connected DAS

In this section, we first briefly discuss the fiber-connected DAS coverage scenario, then present a detailed power model, based on which we introduce the EE of fiber-connected DAS.

2.1. Fiber-Connected DAS

We consider a typical scenario of fiber-connected DAS as depicted in Figure 1, in which a high power remote radio head (H-RRH) guarantees the basic coverage with a number of distributed low power RRHs (L-RRHs) providing complementary coverage for indoor home and office users. Note that HRRH replaces marcoBS while L-RRHs replace femtoBSs in HetNets. Single antenna is assumed at all RRHs and mobile users. L-RRHs are responsible for transmitting and receiving the signals over the air and most of their baseband processing capabilities are moved to the centralized baseband unit (BBU), except for radio frequency (RF) amplifier and electronic-optical conversion. The radio signal between L-RRHs and BBU will be carried through optical fibers, where common public radio interface (CPRI) is considered as the optical interface in this paper. The perfect CSI is assumed available at the BBU.

2.2. Power Model

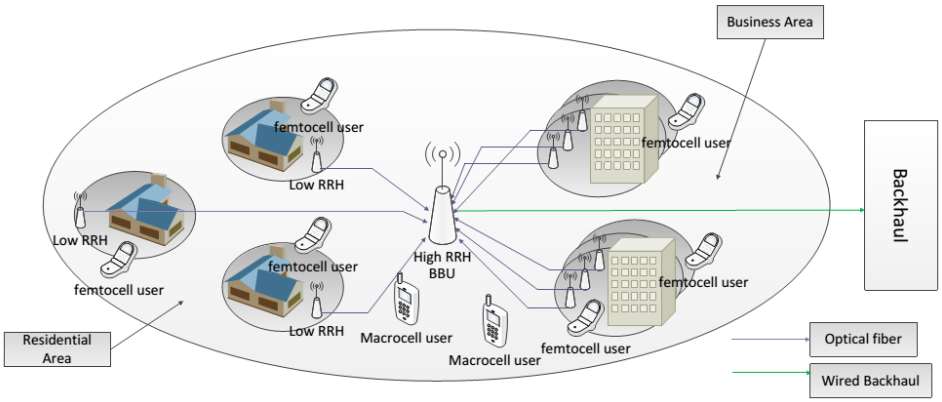

Figure 1. Network Coverage

The potential energy conservation benefits of fiber-connected DAS compared with conventional macro/femto two-tier architecture of HetNets come from two perspectives: One is the mitigated interference by cooperative transmission and the thereby reduced transmission power in the H-RRH which consumes much more power than LRRHs. The other is the less power consumed at inactive L-RRHs due to the joint processing of information at central BBU. Note that all RRHs are not always active at the same time due to the small number of serving users in a femto-cell area.

To demonstrate these advantages, in this subsection we develop a detailed power consumption model by extending the power model of macro-/femtoBS in EARTH project [10] to accommodate H-/L-RRH and BBU in fiber-connected DAS. The power consumption in our model is comprised of four components: digital baseband (BB), power amplifier (PA), analog RF and system overhead, which are further, decomposed by sub-components and calculated as in Table I/II/III/IV. In the following, we detail the power consumption of each component.

2.2.1. Digital baseband processing: The power consumption of digital baseband processing, denoted by P_{BB}, is given by

$$P_{\mathrm{BB}} = P_{\mathrm{S}}(1+\eta_{\mathrm{Leak}}) \tag{1}$$

in which η_{Leak} accounts for complementary metal-oxide-semiconductor (CMOS) leakage current and is fixed at 10% based on 65nm CMOS technology [11]. P_{S} is the sum of all subcomponents corresponding to BB listed in the second column in Table I.

$$P_{\mathrm{S}} = P_{\mathrm{DPD}} + P_{\mathrm{Filter}} + P_{\mathrm{OFDM}} + P_{\mathrm{FD,lin}} + P_{\mathrm{FD,nl}} + P_{\mathrm{CPRI}} + P_{\mathrm{FEC}} + P_{\mathrm{CPU}} \tag{2}$$

In calculating the power consumption of each subcomponent, its computation complexity is first estimated in Giga-Operation Per Second (GOPS), and then GOPS is transformed into watt by multiplying a technology-dependent factor, which is set at 120 GOPS/watt when dedicated processors are used.

Among these subcomponents, the power consumption of CPRI and DPD are dominant. The CPRI energy consumption occurs at both RRH and BBU sides and therefore increases in proportion to the number of active RRHs (we assume that CPRI at inactive RRHs consume negligible energies). According to commercially available chip manuals [12-13], each CPRI channel consumes 1.5 watt. Regarding other baseband processing subcomponents, the power consumption of BBU is almost equal to that of macroBS except nonlinear FD processing $P_{\mathrm{FD,nl}}$, which may require intensive computations by

massive MIMO processing at a large number of RRHs and will incur large baseband power consumption in fiber-connected DAS.

Table 1. Power Consumption Components of BB (macro-/femtoBS data are from [10])

Subcomponent	BBU	H-RRH	L-RRJ	MacroBS	FemtoBS
DPD(digital pre-distortion)	0	160	0	160	0
Filter(digital up/down-sampling and filtering)	0	200	100	200	100
CPRI	180	360	180	360	0
OFDM	30	0	0	80	60
FD(frequency domain) Linear	30	0	0	30	20
FD nonlinear	Pre-coding dependent	0	0	10	5
FEC(forward error correction)	20	0	0	20	20
CPU	0	200	20	200	20

2.2.2. PA: The power consumption of PA is given by [10]

$$P_{\mathrm{PA}} = N_{\mathrm{TX}} \frac{P_{\mathrm{TX}}}{\eta_{\mathrm{PA}}(1-\sigma_{\mathrm{feed}})} \tag{3}$$

Where N_{TX} is the number of antennas participating in MIMO transmission; P_{TX} is the antenna transmission power; η_{PA} is the PA efficiency; σ_{feed} is the feeder loss, which is only applicable to the macroBS because the PA in the H-RRH is mounted close to the antenna for passive cooling.

Table 2. Power Consumption Components of PA (macro-/femtoBS data are from [10])

Subcomponent	BBU	H-RRH	L-RRJ	MacroBS	FemtoBS
Maximum transmit power	-	46 dBm	20 dBm	46 dBm	20 dBm
Power-amplifier efficiency		31.1%	4.4%	31.1%	4.4%
Feeder loss		-	0	50	0

2.2.3. RF: As all BSs/RRHs share the same RF structure, we calculate the power consumption of RF based on the specific amount of power each sub-component consumes and an overall downscaling factor which reduces the power on femtoBSs/L-RRHs due to less constraining specifications and different hardware implementation of smaller cells. Note that BBU doesn't serve any RF part.

Table 3. Power Consumption Components of RF (macro-/femtoBS data are from [10])

Subcomponent	BBU	H-RRH	L-RRJ	MacroBS	FemtoBS
IQ modulator	-	1	1	1	1
Variable attenuator		0.01	0	0.01	0
Buffer		0.3	0	0.3	0
Forward Voltage-Controller Oscillator(VCO)		0.17	0.17	0.17	0.17
Feedback VCO		0.17	0	0.17	0
Feedback mixer		1	0	1	0
Clock generation and buffering		0.99	0.99	0.99	0.99
Digital-to-Analog(DA) converter		1.37	0.2	1.37	0.2
AD converter		0.73	0.14	0.73	0.14
Downscaling factor		1	12	1	12

2.2.4. System overhead: We mainly consider three subcomponents that are related to the system powering, i.e., AC/DC and DC/DC conversion as well as cooling and compute power consumption as a fixed overhead linearly depending on the total power of the rest of base station. Thus we have:

$$P_{\text{overhead}} = (P_{\text{BB}} + P_{\text{RF}} + P_{\text{PA}}) \times ((1+\eta_{\text{cool}})(1+\eta_{\text{dcdc}})(1+\eta_{\text{acdc}}) - 1) \quad (4)$$

The overhead values follow: 10% for η_{cool}; 5% for η_{dcdc}; and 10% for η_{acdc}.

Table IV. Overhead Power Consumption Components (macro-/femtoBS data are from [10])

Subcomponent	BBU	H-RRH	L-RRJ	MacroBS	FemtoBS
Cooling	10%	0	0	10%	0
DC(direct current)/DC	5%	5%	5%	5%	5%
AC(alternating current)/DC	10%	10%	10%	10%	10%

In sum, we can observe that digital baseband and PA are major contributors. The analog RF component P_{RF} only consumes 0.2 watt at a femtoBS and 5.7 watt at the macroBS. The system overhead P_{overhead} adds approximately 25% more energy consumptions on top of other three components. Note that active cooling only occurs at the macroBS and the BBU.

2.3. EE of Fiber-connected DAS

In demonstrating Green radio, EE of a wireless access network is introduced, which is the ratio of data transmission rate R to the total power consumption P_{total} : (unit: bits/Joule).

$$\eta_{\text{EE}} = \frac{R}{P_{\text{total}}} = \frac{R}{P_{\text{BB}} + P_{\text{RF}} + P_{\text{PA}} + P_{\text{overhead}}} \quad (5)$$

3. Proposed Scheme

In this section, we show how the cooperative transmission in fiber-connected DAS can mitigate interference, thus increasing the downlink throughput while reducing transmission power. Then we propose a simple but efficient pre-coding scheme to drop the computation complexity associated with interference mitigation and cooperative transmission.

3.1. Cooperation and its computation complexity

In the macro/femto network architecture, macroBS or femtoBS may cause unexpected interference without proper coordination, because they might transmit their signal to users independently. The large transmission power difference between macroBS and femtoBS, *e.g.*, 46 dBm vs. 20 dBm, also imposes another difficulty on controlling the interference.

In the fiber-connected DAS architecture, however, the whole channel information between users and RRHs, which is referred to as a full channel matrix, is available at the BBU. Particularly, this makes multiple-input multiple-output (MIMO) transmission techniques possible, which can increase the SE. However, the MIMO transmissions may require complicated calculation at the BBU regarding the beam-forming and the power allocation for each RRH. Note that the power consumption is closely related to this computation complexity. Thus, although the BBU is able to support high complexity computations, it needs to control the explosive computation complexity to increase EE.

3.2. Proposed Scheme

In this subsection we present a simple yet efficient scheme to reduce the aforementioned complexity for the zero-forcing beam-forming (ZFBF) at BBU.

In wireless communication systems, the number of active users (or corresponding RRHs) may vary over time. Hence, we use $\mathbf{S}_t$ to denote the active user set at time t. Let $\mathbf{H}(\mathbf{S}_t)$ be downlink channel matrix between the users in $\mathbf{S}_t$ and their serving RRHs. As in HetNets, a user is served by a H-RRH/LRRH. In order to perform ZFBF, channel matrix inversion (MI) is calculated at the BBU which is given as

$$\mathbf{G}(\mathbf{S}_t) = \mathbf{H}^{-1}(\mathbf{S}_t) \tag{6}$$

Moreover, a power allocation procedure is additionally required due to the uneven elements in $\mathbf{G}(\mathbf{S}_t)$. Boccardi and Huang [14] proposed a power allocation procedure to maximize the sum throughput while meeting the per-antenna power constraint, which solves the following convex optimization problem:

$$\max \sum_{k=1}^{|S_t|} \log(1+s_k / N_0) \qquad \text{s.t.} \begin{cases} s_k \geq 0, k = 1, \cdots, |\mathbf{S}_t|, \\ \sum_{k=1}^{|S_t|} |g_{mk}|^2 s_k \leq P_m, m = 1, \cdots, |\mathbf{S}_t|. \end{cases} \tag{7}$$

where $|g_{mk}|$ is the (m,k) th element of $\mathbf{G}(\mathbf{S}_t)$, $|g_{mk}|^2 \upsilon_k$ and P_m are respectively the power allocated to the m-th RRH and the corresponding power constraint, and $|\mathbf{S}_t|$ denotes the cardinality of the set $\mathbf{S}_t$. ZFBF requires the BBU to perform the MI as in (6) and the power allocation under the per-antenna power constraint as in (7) which requires a high complexity and accompanies a high power consumption due to the computation

In order to reduce the accompanying complexity, we introduce the following two procedures:

3.2.1. Matrix inversion (MI): We make the channel matrix sparse to reduce the complexity related to the channel matrix inversion (MI):

First, the channel gains between users and L-RRHs located in different buildings are assumed to be 0. Such relaxation is possible due to the large penetration losses in signal strength of outer walls, *e.g*. 20dB loss for each outer wall.

Second, only K_1 largest channel gains remain between the L-RRHs to the macrocell user, while the other elements are forced to be zeros; Third, Only K_2 largest channel gains remain between the H-RRH to the femto-cell users, while the other elements are also forced to be zeros. The two relaxations are reasonable due to the geometrically distributed property of RRHs and users. The selection of K_1 and K_2 depends on the computational efficiency of the BBU and the deployment density of RRHs.

3.2.2. Stream Power allocation (SPA): We use the following stream power allocation (SPA) scheme to reduce the computation at the BBU.

First, we multiply the channel gains between the H-RRH and all active users by $\sqrt{c}$, where $c = P_{\mathrm{H}} / P_{\mathrm{L}}$. Then, we make the transmit power of the H-RRH identical to L-RRHs and relax the per-antenna power constraint to sum-power constraint, which can be solved by water-filling algorithm with much less complexity;

Second, we multiply a factor λ to all the allocated RRH power P_a so that the allocated power of all RRHs are not larger than the power constraint of L-RRHs, i.e.,

$$\lambda P_a \leq P_{\mathrm{L}}, m = 1, \cdots, |\mathbf{S}_t| \tag{8}$$

Finally we multiply c back to power allocated to the H-RRH. In the proposed power allocation procedure, if we do not apply the first and last normalization procedure, the allocated power to the L-RRHs after the water-filling in the second procedure would almost be zero since the power of H-RRH is much larger than that of L-RRH which may affect the computational precision.

3.2.3. Complexity and Power Consumption of MI and SPA: For MI, the channel matrix after relaxation, denoted as $\hat{\mathbf{H}}(\mathbf{S}_t)$, only has $K_1 + K_2 + N_1 + N_2 M^2 + 1$ non-zero elements. Without such relaxation, the original channel matrix $\mathbf{H}(\mathbf{S}_t)$ has $(N_1 + N_2 M + 1)^2$ non-zero elements, which is much larger than $K_1 + K_2 + N_1 + N_2 M^2 + 1$ especially with large N_1 and N_2. For SPA, the water-filling process is much less complicated than the optimal power allocation scheme that solves a convex optimization problem as in (2) in each channel realization.

The detailed computation complexity of MI and SPA, measured in GOPS (Giga-Operations Per Second), will be transformed from the floating-point operation (flop) count by considering how frequently MI and SPA operations are needed in downlink transmission. In the downlink of a 10-MHz FDD-LTE system, there are 14,000 OFDM symbols being transmitted every second and 600 sub-carriers being used across the channel. With these configurations, we can translate flops into GOPS and then obtain the power consumption contributed by MI and SPA through the developed power model. The exact flop count of MI and SPA is determined by enumerating non-zero entries that participate in the calculation, as summarized in Table V.

Table V. Floating-point Operation (flop) Count of MI and SPA

Component	flop count
MI	$\sum_{k=1}^{I} v_k \cdot \sum_{k=1}^{2I} v_k + 2\sum_{k=1}^{N_2} v_k^3$
SPA	$2\sum_{k=1}^{2I} v_k \cdot \sum_{k=1}^{I} v_k + 2\sum_{k=I+1}^{N_2} v_k^2$

Note: v_k is the number of active antennas in the k-th building with multiple L-RRHs; I is the number of entries being kept in macroBS to femtocell users matrix and in macrocell user to other femtoBSs matrix (excluding the main diagonal one).

4. Numerical Results

In this Section, we present simulation results to demonstrate the effectiveness of our proposed scheme from two perspectives: SE and EE.

Fiber-connected DAS with an H-RRH and multiple L-RRHs is compared to a macro/femto architecture consisting of multiple femtoBSs in a macroBS, referred as HetNet for simplicity. The H-RRH (or macroBS) has a transmission coverage of 500m-radius, where 60 houses of one-story and 15 four-story office buildings are uniformly distributed within the coverage area. An L-RRH (or femtoBS) is located at the center of each floor of a house or an office building and has a coverage of 30m-radius. The H-RRH and L-RRHs (or macro- and femtoBSs) have a bandwidth of 10 MHz in 2 GHz band. The transmit power constraints for HRRH and L-RRHs (or the macro- and femtoBSs) are set to 46 dBm and 20 dBm, respectively. Over downlink, the H-RRH and L-RRHs (or the macro and femto BSs) transmit signals to users which are randomly located under the coverage range of H-RRH and L-RRHs (or the macro and femto cell). The 3GPP dual-strip model in [15] (Table A. 2.1.1.2-8) is used as the channel model in the simulations, where the penetration losses of the signal strength due to the inner and outer walls are 5 dB and 20 dB, respectively. The Shannon capacity achievable coding scheme is assumed in this section.

4.1. Spectral Efficiency

An activity ratio of each L-RRH (or femtoBS) reflects the phenomenon that the activities of house and office users vary during a day, *e.g.*, traffic migration. If the activity ratio of an L-RRH is set to p, then the user located in the coverage area of the L-RRH receives signals with the probability p at each time slot. A larger p in indicates the use is more active in communicating with its L-RRH. The sum of activity ratios of L-RRH in house and office users are set to 1. In day time, the L-RRHs in the office building may be more active while the L-RRHs in the house buildings are more active in night time. Since the H-RRH (or macroBS) covers the whole area, the activity ratio of H-RRH (or macroBS) is assumed to be 1, *i.e.*, always active.

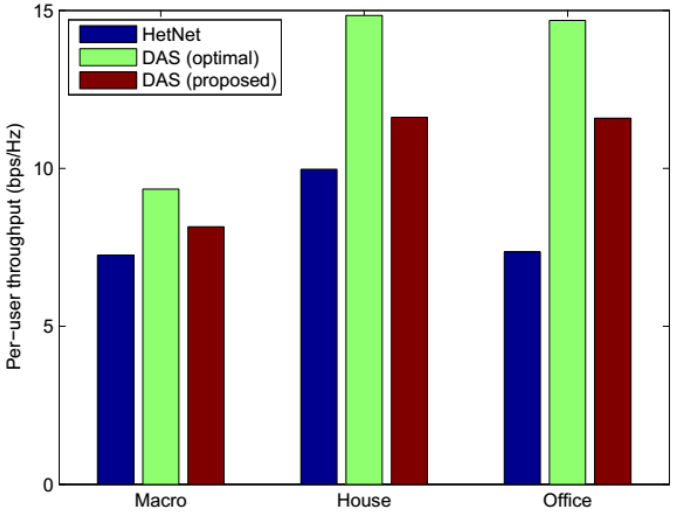

Figure 2. Per-user Throughput vs. Network Architecture

Figure 2 compares the per-user throughput of fiber-connected DAS with optimal power allocation [14] and with the proposed scheme against that of HetNet, when the activity ratios of house and office users are both set to 0.5. For the proposed scheme, K_1 and K_2 are set to 3. It is notable the optimal scheme has high computation complexity as it applies full channel matrix information to perform ZFBF as well as solves a complicated convex optimization problem to calculate the allocated power for each RRH. We can observe fiber-connected DAS improves throughput of macrocell, house and office users compared to those in HetNet.

Figure 3 also compares the per-user throughput, when the activity ratio of house users varies. In the X-label of the figure, if the access ratio of house users is p, the access ratio of office users is $1-p$. Since the optimal scheme incurs a huge power consumption caused by high computation complexity at the BBU, we will present in the rest of the paper only the performance of fiber-connected DAS with the proposed scheme, referred to as F-DAS for simplicity. While F-DAS shows higher throughput than HetNet, the throughput at the H-RRH decreases as the activity of house users increases in both architecture. This is due to the fact that, compared with the office buildings, L-RRHs among the houses are located far apart and would therefore cause strong interference with macrocell users. The office users show a higher throughput as their activity ratio decreases, because the interference within the same office building is consequently reduced. Due to the high penetration loss of the outer walls of isolated house users, the interferences among house users become negligible, which results in the constant

throughput of house users regardless of their activity ratio variation. Hence, F-DAS can give the office users higher throughput than the house users.

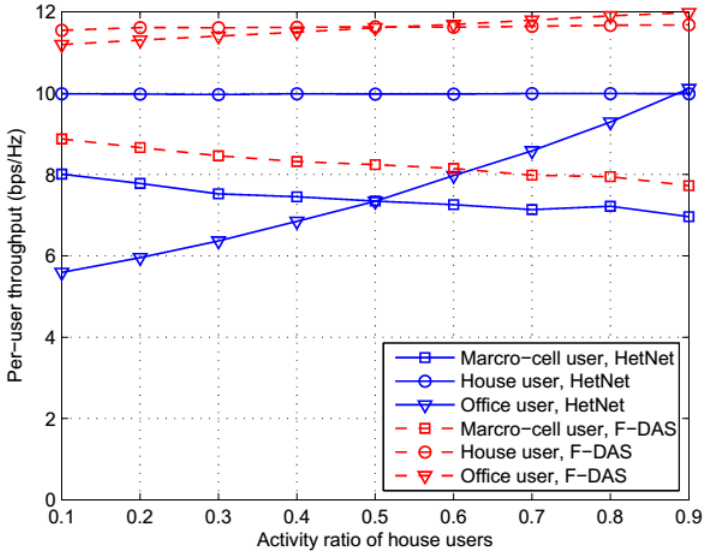

Figure 3. Per-user Throughput vs. Activity Ratio of House

4.1. Energy Efficiency

Figure 4 shows the transmission power consumption of FDAS normalized with respect to HetNet. Since the normalized transmission power consumption is less than 1 in all cases, it can be concluded that users in F-DAS require much less power than those in HetNet. It is notable that the transmission power of L-RRHs for users in the houses and offices in FDAS is less than 70% of that of HetNet. Combining the results in Figure 3 and Figure 4, we can see that F-DAS provides a higher throughput even with a smaller transmission power consumption compared to HetNet.

Figure 5 shows the total power consumption as well as EE. We can see that F-DAS consumes less power than HetNets, especially under high activity ratio of house users. Under low activity ratio of house users (or high activity ratio of office users), however, the total power consumption of F-DAS is similar to that of HetNets. This is because the interference within an office building is dominant over the interference among the houses and the power spent on mitigating the interference is increased along with high activity ratio of office users. In fact, the digital baseband processing at BBU takes almost 40% of the total power consumption in F-DAS when the activity ratio of house user is 0.5, and would consume more when the activity ratio of office users increases. Thus, reducing power consumption related to computation complexity at BBU would be an interesting and worthwhile research issue. It should be noted that F-DAS always shows much higher EE for any activity ratio of house user.

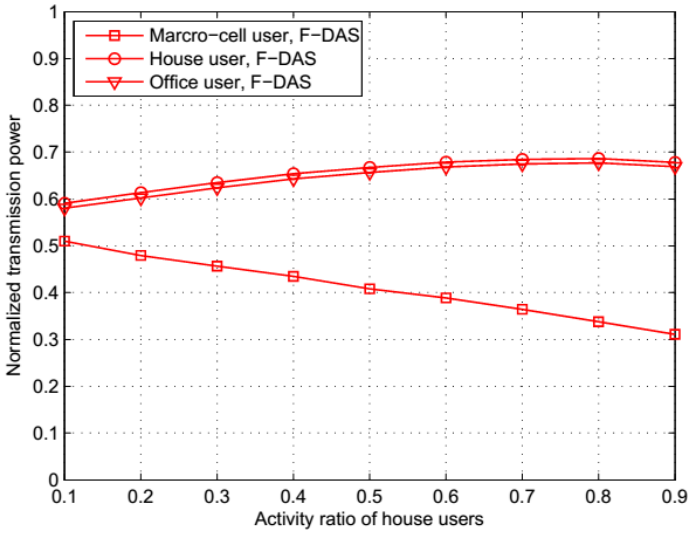

Figure 4. Normalized Transmission Power vs. Activity Ratio of House Users

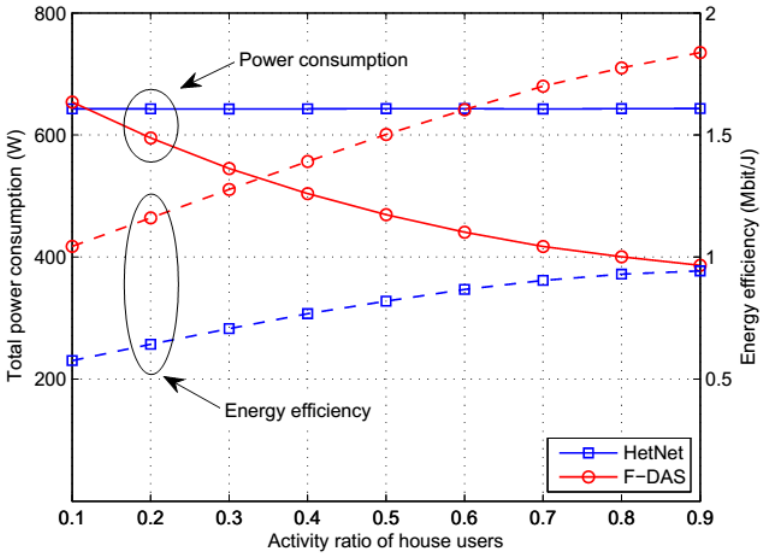

Figure 5. Total Power Consumption and Energy Efficiency vs. Activity Ratio of House Users

5. Conclusion

The power consumption of traditional wireless networks and its impacts on environmental protection are of growing concerns. This paper focused on the SE and EE of the fiber-connected DAS architecture in HetNet. The SE advantage was achieved by cooperative transmission among RRHs. The EE performance was improved by reducing the cooperation associated power consumption through proposed computational efficient pre-coding scheme. A detailed power model was further developed to benchmark the various sources of energy consumption in fiber-connected DAS. Through detailed

simulation, this paper demonstrated the energy efficient application of the fiber-connected DAS with proposed pre-coding scheme in HetNet.

References

[1] Cisco, "Cisco visual networking index: Global mobile data traffic forecast update, 2010-2015", White paper, **(2011)**, pp. 1-40.
[2] H. Li, J. Hajipour, A. Attar and V. C. M. Leung, "Efficient HetNet implementation using broadband wireless access with fiber-connected massively distributed antennas architecture", IEEE Wireless Communications, vol. 18, no. 3, **(2011)**, pp. 72-78.
[3] X. -H. You, D. -M. Wang, B. Sheng, X. -Q. Gao, X. -S. Zhao and M. Chen, "Cooperative distributed antenna systems for mobile communications [Coordinated and Distributed MIMO]", IEEE Wireless Communications, vol. 17, no. 3, **(2010)**, pp. 35-43.
[4] D. Gesbert, S. Hanly, H. Huang, S. Shamai Shitz, O. Simeone and W. Yu, "Multi-cell MIMO cooperative networks: a new look at interference", IEEE Journal of Selected Areas on Communication, vol. 28, no. 9, **(2010)**, pp. 1380-1408.
[5] Attar, H. Li and V. C. M. Leung, "Green last mile: how fiber-connected massively distributed antenna systems can save energy", IEEE Wireless Communications, vol. 18, no. 5, **(2011)**, pp. 66-74.
[6] He, B. Sheng, P. Zhu, X. You and G. Y. Li, "Energy- and spectral-efficiency tradeoff for distributed antenna systems with proportional fairness", IEEE Journal of Selected Areas on Communication, vol. 31, no. 5, **(2013)**, pp. 894-902.
[7] X. Chen, X. Xu and X. Tao, "Energy efficient power allocation in generalized distributed antenna system", IEEE Communication Letter, vol. 16, no. 7, **(2012)**, pp. 1022-1025.
[8] Y. Lin, Z. Zhu, Q. Wang and R. K. Sabhikhi, "Wireless network cloud: Architecture and system requirement", IBM Journal of Research and Development, vol. 54, no. 1, **(2010)**, pp. 1-12.
[9] China Mobile Research Institute, "C-ran: The road towards green ran", White Paper, Ver 2.5.0, **(2011)**.
[10] G. Auer, "D2.3: Energy efficiency analysis of the reference systems, areas of improvements and target breakdown", INFSO-ICT-247733 Earth (Energy Aware Radio and NeTwork TecHnologies), Tech. Rep., **(2010)**.
[11] C. Desset, "Flexible power modeling of LTE base stations", 2012 IEEE Wireless Communications and Networking Conference (WCNC), **(2012)**, pp. 2858-2862.
[12] Texas Instruments, "TLK6002: Dual Channel 0.47Gbps to 6.25Gbps Multi-Rate Transceiver", Texas Instruments SLLSE34A Rev. A, **(2010)**.
[13] Avago Technologies, "Digital Diagnostic SFP, 850nm 3.072/2.4576 Gb/s, RoHS OBSAI/CPRI Compatible Optical Transceiver", Avago Technologies AFBR-57J5APZ, **(2013)**.
[14] F. Boccardi and H. Huang, "Zero-forcing precoding for the MIMO Broadcast Channel under Per-Antenna Power Constraints", IEEE 7th Workshop on Signal Processing Advances in Wireless Communications, **(2006)**, pp. 1-5.
[15] 3GPP, "E-UTRA: Further advancements for E-UTRA physical layer aspects", 3GPP TR 36.814 V9.0.0, **(2010)**.

